Available online at www.sciencedirect.com
ScienceDirect
Journal of Molecular Catalysis A: Chemical 283 (2008) 129–139
JOURNAL OF MOLECULAR CATALYSIS A: CHEMICAL
www.elsevier.com/locate/molcata

Oxidation of adamantane catalysed by imidazolylporphyrinatoiron(III) complexes and structural studies of 5-coordinating iron(III) porphyrin

Yuji Miyazaki, Akiharu Satake *, Yoshiaki Kobuke **

The Graduate School of Materials Science, Nara Institute of Science and Technology (NAIST), Takayama 8916-5, Ikoma, Nara 630-0192, Japan

Received 10 September 2007; received in revised form 17 November 2007; accepted 13 December 2007
Available online 23 December 2007

Abstract

Oxidation of adamantane with phenylperacetic acid was carried out in the presence of three imidazolyltriarylporphyrinatoiron(III) complexes having pentafluorophenyl, phenyl, and mesityl (2,4,6-trimethylphenyl) groups as *meso*-substituents and three corresponding tetraarylporphyrinatoiron(III) complexes. The yield of 1- and 2-adamantanols was 76% in the case of chloro-5-(1-methyl-2-imidazolyl)-10,15,20-tri(pentafluorophenyl)porphyrinatoiron(III) (ImTPFPP–Fe(III)Cl), whereas the yield was only 26% in the case of chloro-5,10,15,20-tetra(pentafluorophenyl)porphyrinatoiron(III) in the presence of 100 eq. *N*-methylimidazole. The apparent effect of the appended imidazolyl group is discussed in terms of a 5-coordinated dimer of ImTPFPP–Fe(III)Cl, which was observed in the ^{1}H and ^{19}F NMR, and UV–vis spectra.

Keywords: Iron porphyrin; Oxidation; Peroxy acid; Imidazole coordination; Supramolecule

1. Introduction

One-oxygen oxidation of inactive C–H bonds has been of great interest in both enzymatic reactions and synthetic organic chemistry [1]. Various metal catalysts have been developed for this purpose and discussed in relation to the excellent activation methods in natural systems [2]. Peroxidases and cytochrome P-450 have been investigated most extensively as one-oxygen oxidation catalysts. Mimics of their structure and function have been examined for nearly three decades, and their development has been a continuing target of active research [3]. The following two basic strategies are proposed for active catalysts: (1) A proximal imidazole group introduced in an iron porphyrin assists heterolytic O–O bond cleavage by the push effect [4]; (2) substituents of *meso*-aryl groups greatly affect the reactivity. For example, pentafluorophenyl and 2,6-dichlorophenyl groups significantly improve the turnover number of catalytic oxidation with the use of peracids and peroxide [5].

We report here a new iron(III) porphyrin catalyst **1** that has one 2-imidazolyl group and three pentafluorophenyl groups at *meso* positions (Fig. 1). Complex **1** is expected to form its dimer **2**, representing the otherwise difficult-to-obtain 5-coordinated iron(III) species. We previously reported such complementary dimers for zinc(II) [6], magnesium(II) [7], cobalt(II), and cobalt(III) imidazolylporphyrin [8], but not iron(III) porphyrin. Catalyst **1** shows good activity for oxidation of adamantane with phenylperacetic acid (PPAA) as the oxidant. We also report structural studies of 5-coordinated dimer **2** by UV–vis as well as ^{1}H and ^{19}F NMR spectroscopy in conjunction with elucidation of the structure of the active catalyst.

2. Experimental

2.1. Materials

All the commercially available chemicals were used directly unless otherwise described. 1-Methylimidazole and CH_2Cl_2 were distilled over CaH_2. Phenylperacetic acid (PPAA) was prepared according to the literature method [9]. 2,4,6-Tri-(*tert*-butyl)phenol (TBPH) was purified by recrystallization from hot

* Corresponding author. Tel.: +81 743 72 6113; fax: +81 743 72 6119.
** Corresponding author. Present address: Institute of Advanced Energy, Kyoto University, Gokasho, Uji 611 0011, Japan. Tel.: +81 774 38 4581; fax: +81 774 38 4577.
E-mail addresses: satake@ms.naist.jp (A. Satake), kobuke@ms.naist.jp, kobuke@iae.kyoto-u.ac.jp (Y. Kobuke).

1381-1169/$ – see front matter © 2007 Elsevier B.V. All rights reserved.
doi:10.1016/j.molcata.2007.12.016

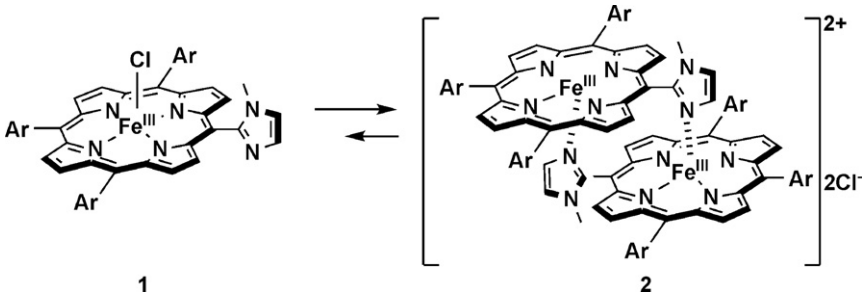

Fig. 1. Chloro(imidazolylporphyrinato)iron(III) **1** and its dimer **2**.

ethanol. Tetra(pentafluorophenyl)porphyrin [10], tetraphenylporphyrin [11], and tetra(mesityl)porphyrin [12] were prepared according to the corresponding literatures.

2.2. Instruments

^{1}H and ^{19}F NMR spectra were measured on a JEOL JNM-ECP 600 spectrometer in $CDCl_3$ or acetonitrile-d_3. ^{1}H chemical shifts were referenced to TMS as the internal standard in the case of $CDCl_3$ solution, and to the residual protons (1.96 ppm) in the case of acetonitrile-d_3 solution. ^{19}F chemical shifts were referenced to trifluoroacetic acid (−76.5 ppm) as the external standard. UV–vis spectra were measured by a Shimadzu UV-3000 PC spectrometer. Fluorescence spectra were recorded on a Hitachi F-4500 spectrometer. MALDI-TOF mass spectra were measured on a Perseptive Biosystems Voyager DE-STR or Shimadzu AXIMA with dithranol as a matrix. High-resolution mass spectra (FAB method, *m*-NBA as a matrix) were measured on a JEOL *M*Station. TLC was operated on glass plates coated with 60 F_{254} (Merck) silica gel. Column chromatography was undertaken using a column packed with silica gel 60 N (Kanto Chemical, spherical, neutral, 63–210 μm). Gas chromatography was carried out on a Shimadzu GC-14B gas chromatograph with an FID detector using a 0.25 mm × 30 m dimethylpolysiloxane capillary column (DB-1, J&W Scientific).

2.3. Porphyrin synthesis

2.3.1. 5-(1-Methyl-2-imidazolyl)-10,15,20-tris(pentafluorophenyl)porphyrin, $ImTPFPPH_2$

1-Methyl-2-imidazolecarboxaldehyde (93.6 mg, 0.85 mmol, 1.0 eq.) and pentafluorobenzaldehyde (500 mg, 2.55 mmol, 3.0 eq.) were dissolved in refluxing propionic acid (50 mL). Pyrrole (228 mg, 3.40 mmol, 4.0 eq.) was then added quickly to the boiling solution. The mixture was heated under reflux for 4 h. The solvent of the reaction mixture was removed by distillation under reduced pressure. The ethyl acetate solution (100 mL) of the residue was washed with saturated aqueous $NaHCO_3$ solution and brine, dried over anhydrous Na_2SO_4, and evaporated under reduced pressure. The crude material included tetraarylporphyrin, target monoimidazolylporphyrin, and other multi-imidazolylporphyrins. The residue was purified by silica gel column chromatography eluting with chloroform/acetone (10/1). The least polar tetraarylporphyrin was eluted first, and then a porphyrin mixture (82.5 mg) containing predominantly the target was followed. Since the mixture included not only the target but also many byproducts having similar polarities, the free base porphyrin was once converted to the zinc form which was less polar than the byproducts due to complementary coordination [7]. A methanol solution saturated with zinc acetate dihydrate (2.0 mL) was added to the chloroform solution (50 mL) of the material and stirred at rt for 5 h. The reaction mixture was washed with saturated aqueous $NaHCO_3$ solution and brine, dried over anhydrous Na_2SO_4, and evaporated under reduced pressure. This residue was purified by silica gel column chromatography eluting with benzene to give a zinc porphyrin mixture (66.6 mg). The methanol solution (2.0 mL) of 35% aqueous HCl (0.5 mL) was added to the chloroform solution (50 mL) of the zinc porphyrin, and stirred at rt for 5 h. The reaction mixture was washed with saturated aqueous $NaHCO_3$ solution and brine, dried over anhydrous Na_2SO_4, and evaporated under reduced pressure. The residue was purified by silica gel column chromatography eluting with chloroform/acetone (9/1) to give pure free base porphyrin as purple solids (61.5 mg, 0.0692 mmol, 8.1%). ^{1}H NMR (600 MHz, $CDCl_3$) δ −2.91 (s, 2H, NH), 3.47 (s, 3H, imidazole-Me), 7.52 (d, J = 1.2 Hz, 1H, imidazole), 7.70 (d, 1H, J = 1.2 Hz, imidazole), 8.88 (br, 2H, pyrrole), 8.91 (br, 4H, pyrrole), 8.94 (br, 2H, pyrrole); ^{19}F NMR (564 MHz, $CDCl_3$) δ −162.43 (ddd, J = 24.3, 20.9, 7.3 Hz, 2F, phenyl-*m*), −162.27 (ddd, J = 24.3, 24.3, 10.2 Hz, 1F, phenyl-*m*), −162.07 (ddd, J = 24.3, 24.3, 10.2 Hz, 1F, phenyl-*m*), −161.93 (ddd, J = 24.3, 20.9, 7.3 Hz, 2F, phenyl-*m*), −152.20 (td, J = 20.9, 10.7 Hz, 2F, phenyl-*p*), −152.16 (td, J = 24.3, 7.3 Hz, 1F, phenyl-*p*), −137.60 (dd, J = 24.3, 10.7 Hz, 2F, phenyl-*o*), −137.51 (dd, J = 24.3, 7.3 Hz, 1F, phenyl-*o*), −137.04 (dd, J = 24.3, 10.7 Hz, 2F, phenyl-*o*), −137.03 (dd, J = 24.3, 7.3 Hz, 1F, phenyl-*o*); MALDI-TOF MS *m*/*z* 889.6 (M + H$^+$), Calcd for $C_{42}H_{15}F_{15}N_6$, 888.1; HRMS *m*/*z* 889.1198 (M + H$^+$), Calcd for $C_{42}H_{16}F_{15}N_6$, 889.1197; UV–vis ($CHCl_3$) λ_{max} (Abs. ratio) 415(1), 507(0.074), 585(0.024), 637(0.0029) nm; fluorescence (λ_{Ex} 415 nm, $CHCl_3$) λ_{Em} 641, 710 nm.

2.3.2. 5-(1-Methyl-2-imidazolyl)-10,15,20-triphenylporphyrin, $ImTPPH_2$

1-Methyl-2-imidazolecarboxaldehyde (5.0 g, 45.4 mmol, 1.0 eq.) and benzaldehyde (16.9 g, 159 mmol, 3.5 eq.) were dissolved in refluxing propionic acid (700 mL). A solution of

pyrrole (13.7 g, 204 mmol, 4.5 eq.) in propionic acid (300 mL) was then added slowly to the solution under reflux. After the addition, the reaction mixture was refluxed for further 30 min. Most of the solvent of reaction mixture was removed with distillation under reduced pressure. The ethyl acetate solution (300 mL) of the residue was washed with saturated aqueous $NaHCO_3$ solution and brine, dried over anhydrous Na_2SO_4, and evaporated under reduced pressure. The residue was purified by silica gel column chromatography eluting with chloroform/acetone (9/1) to give a purple solids (1.55 g, 2.51 mmol, 5.5%). ^{1}H NMR (600 MHz, $CDCl_3$) δ −2.77 (s, 1H, NH), 3.44 (s, 3H, imidazole-Me), 7.47 (d, J = 1.8 Hz, 1H, imidazole), 7.67 (d, J = 1.8 Hz, 1H, imidazole), 7.73–7.81 (m, 9H, phenyl), 8.15–8.26 (m, 6H, phenyl), 8.78 (d, J = 4.2 Hz, 2H, pyrrole), 8.84 (s, 4H, pyrrole), 8.90 (d, J = 4.2 Hz, 2H, pyrrole); MALDI-TOF MS m/z 619.2 ($M+H^+$), Calcd for $C_{42}H_{30}N_6$, 618.3; HRMS m/z 618.2534 (M^+), Calcd for $C_{42}H_{30}N_6$, 618.2532; UV–vis ($CHCl_3$) λ_{max} (Abs. ratio) 418(1), 515(0.054), 550(0.019), 588(0.018), 644(0.0086) nm; fluorescence (λ_{Ex} 418 nm, $CHCl_3$) λ_{Em} 647, 711 nm.

2.3.3. 5-(1-Methyl-2-imidazolyl)-10,15,20-trimesitylporphyrin, *ImTMPH$_2$*

Since the title compound was scarcely obtained by Adler method using benzaldehyde and imidazolecarboxaldehyde in propionic acid, modified dipyrromethane method was applied. Mesityldipyrromethane [13] (528 mg, 2.0 mmol, 2.0 eq.) and mesitaldehyde (148 mg, 1.0 mmol, 1.0 eq.) were dissolved in chloroform (100 mL). BF_3 OEt_2 (260 mg, 2.0 mmol, 2.0 eq.) was added at rt and stirred for 1 h. At this stage, tetrapyrrol was detected by MALDI-TOF mass. This reaction mixture was passed through a column filled with solid $NaHCO_3$ eluting with chloroform (100 mL) to neutralize the acid. To the eluent, 1-methyl-2-imidazolecarboxaldehyde (110 mg, 1.0 mmol, 1.0 eq.) and trifluoroacetic acid (228 mg, 2.0 mmol, 2.0 eq.) was added, and the mixture was stirred for 5 h. The mixture was washed with saturated aqueous $NaHCO_3$ solution and brine, dried over anhydrous Na_2SO_4, and evaporated under reduced pressure. The residue was roughly purified by silica gel column chromatography eluting with chloroform/acetone (9/1) to give a porphyrin mixture (41.2 mg) containing predominantly the target. For further purification, the mixture was converted to zinc porphyrin similarly to the case of **ImTPFPPH$_2$**. After purification, the zinc porphyrin (31 mg) was demetalated to give the title compound **ImTMPH$_2$** as purple solids (27 mg, 0.0362 mmol, 3.6%). ^{1}H NMR (600 MHz, $CDCl_3$) δ −2.56 (s, 1H, NH), 1.79 (s, 6H, mesityl-Me), 1.84 (s, 3H, mesityl-Me), 1.89 (s, 6H, mesityl-Me), 1.93 (s, 3H, mesityl-Me), 2.62 (s, 9H, mesityl-Me), 3.47 (s, 3H, imidazole-Me), 7.23–7.26 (m, 2H, mesityl), 7.27–7.29 (m, 4H, mesityl), 7.45 (s, 1H, imidazole), 7.64 (s, 1H, imidazole), 8.63 (br-s, 2H, pyrrole), 8.65 (br-s, 2H, pyrrole), 8.72 (br-s, 2H, pyrrole); MALDI-TOF MS m/z 745.2 ($M+H^+$), Calcd for ($C_{51}H_{48}N_6$) 744.4; UV–vis ($CHCl_3$) λ_{max} (Abs. ratio) 420(1), 516(0.052), 550(0.016), 589(0.018), 645(0.0078) nm; fluorescence (λ_{Ex} 420 nm, $CHCl_3$) λ_{Em} 647, 714 nm.

2.3.4. Chloro[5-(1-methyl-2-imidazolyl)-10,15,20-tripentafluorophenylporphyrinato]iron(III), *ImTPFPP–Fe(III)Cl*

ImTPFPPH$_2$ (61.5 mg, 0.0692 mmol, 1.0 eq.) and excess iron(II) chloride tetrahydrate (138 mg, 0.692 mmol, 10 eq.) were dissolved in acetonitrile (20 mL) at rt. The mixture was heated under reflux for 5 h. The solvent was evaporated under reduced pressure. The chloroform solution (50 mL) of the residue was washed with 1 M HCl and brine, dried over anhydrous Na_2SO_4, and evaporated under reduced pressure. The product was purified by reprecipitation with chloroform/hexane. The pure compound was obtained as dark green solids (53.3 mg, 0.055 mmol, 79%). MALDI-TOF MS m/z 942.7(M^+), 978.2 ($M+Cl+H^+$), 1885.0 ($2M+H^+$), Calcd for $C_{42}H_{13}F_{15}FeN_6$, 942.0; HRMS m/z 943.0394 ($M+H^+$), Calcd for $C_{42}H_{14}F_{15}FeN_6$, 943.0390; UV–vis (acetonitrile) λ_{max} nm (M^{-1} cm^{-1}) 395 (65,900), 505 (8800), 632 (4300), UV–vis (acetonitrile + 70 eq. 1MeIm) λ_{max} nm (M^{-1} cm^{-1}) 411 (124,000), 542 (8500), UV–vis ($CHCl_3$) λ_{max} (Abs. ratio) 357(0.55), 413(1), 505(0.12), 626(0.053) nm.

2.3.5. Chloro[5-(1-methyl-2-imidazolyl)-10,15,20-trisphenylporphyrinato]iron(III), *ImTPP–Fe(III)Cl*

Reaction conditions were almost same as **ImTPFPP–Fe(III)Cl** except for $CHCl_3$ as solvent instead of acetonitrile. From **ImTPPH$_2$** (200 mg, 0.323 mmol, 1.0 eq.), the title compound was obtained as black solids (194 mg, 0.274 mmol, 84%). ^{1}H NMR (600 MHz, $CDCl_3$) δ −5.88 (br-s, 3H, phenyl), 6.71 (br-s, 2H, phenyl), 6.92 (br-s, 3H, imidazole-Me), 7.11 (br-s, 1H, phenyl), 8.85 (br-s, 3H, phenyl), 11.00 (br-s, 3H, phenyl), 11.93 (br-s, 1H, imidazole), 12.23 (br-s, 3H, phenyl), 14.37 (br-s, 1H, imidazole), 76.83 (br-s, 2H, pyrrole), 77.88 (br-s, 2H, pyrrole), 82.07 (br-s, 4H, pyrrole); MALDI-TOF MS m/z 672.5 (M^+), 708.0 ($M+Cl+H^+$), 1345.6 ($2M+H^+$) Calcd for $C_{42}H_{28}FeN_6$, 672.2; HRMS m/z 673.1795 ($M+H^+$), Calcd for $C_{42}H_{29}FeN_6$, 673.1804; UV–vis ($CHCl_3$) λ_{max} (Abs. ratio) 379(0.54), 417(1), 510(0.11), 580(0.025) nm.

2.3.6. Chloro[5-(1-methyl-2-imidazolyl)-10,15,20-trismesitylporphyrinato]iron(III), *ImTMP–Fe(III)Cl*

Reaction conditions were almost same as **ImTPFPP–Fe(III)Cl** except for toluene for reaction solvent, and diethylether/hexane for reprecipitation. From **ImTMPH$_2$** (20 mg, 0.0268 mmol, 1.0 eq.), the title compound was obtained as light brown solids (18.8 mg, 0.0225 mmol, 84%). ^{1}H NMR (600 MHz, $CDCl_3$) δ −3.16 (br-s, 9H, mesityl-Me), 3.77 (s, 3H, imidazole-Me), 3.88 (br-s, 9H, mesityl-Me), 6.16 (br-s, 9H, mesityl-Me), 11.53–15.08 (m, 8H, mesityl-Me, imidazole), 3.16 (br-s, 9H, mesityl-Me), 75.88 (br-s, 2H, pyrrole), 77.17 (br-s, 2H, pyrrole), 81.00 (br-s, 2H, pyrrole), 81.64 (br-s, 2H, pyrrole); MALDI-TOF MS m/z 798.4 (M^+), 834.3 ($M+Cl+H^+$), 1668.7 ($2M+H^+$), Calcd for $C_{51}H_{46}FeN_6$, 798.3; HRMS m/z 799.3218 ($M+H^+$), Calcd for $C_{51}H_{47}FeN_6$, 799.3213; UV–vis ($CHCl_3$) λ_{max} (Abs. ratio) 377(0.52), 418(1), 508(0.12), 662(0.027) nm.

2.3.7. Perchloro[5-(1-methyl-2-imidazolyl)-10,15,20-triphenylporphyrinato]iron(III), ImTPP–Fe(III)ClO_4

CAUTION! Although we encountered no problems, care should be taken when using the potentially explosive perchlorate compounds.

ImTPP–Fe(III)Cl (164 mg, 0.232 mmol, 1.0 eq.) was dissolved in THF (20 mL). $AgClO_4$ (96.2 mg, 0.464 mmol, 2.0 eq.) was added to the solution, and the mixture was stirred at rt for 1 h. Precipitates were filtered on membrane filter (0.1 μm, polyvinylidene fluoride), and the filtrate was evaporated. The residue was purified by reprecipitation with hot toluene to give red black solids (199 mg, 0.258 mmol, 95%). MALDI-TOF MS *m/z* 672.2 (M^+), 1345.2 ($2M + H^+$), Calcd for $C_{42}H_{28}FeN_6$, 672.2; UV–vis ($CHCl_3$) λ_{max} (Abs. ratio) 400(1), 523(0.081), 654(0.014) nm.

2.3.8. Perchloro[5-(1-methyl-2-imidazolyl)-10,15,20-trismesitylporphyrinato]iron(III), ImTMP–Fe(III)ClO_4

In accordance with the procedure for **ImTPP–Fe(III)ClO_4**, the title compound (11.6 mg, 0.0129 mmol, 90%) was obtained as red brown solids from **ImTMP–Fe(III)Cl** (12 mg, 0.0144 mmol). MALDI-TOF MS *m/z* 798.4 (M^+), Calcd for $C_{51}H_{46}FeN_6$, 798.3; UV–vis ($CHCl_3$) λ_{max} (Abs. ratio) 396(1), 517(0.071), 689(0.0076) nm.

2.4. Catalytic reaction

2.4.1. Catalytic oxidation of TBPH with PPAA

Iron(III) porphyrin (0.10 μmol) was placed in a test tube fitted with a rubber septum. The inside was replaced with Ar atmosphere. A TBPH solution (25 mM in CH_2Cl_2, 0.8 mL, 20 μmol) was added to the test tube. Subsequently, a mixture (0.2 mL) of PPAA (5.0 mM, 1.0 μmol) and diethyleneglycol diethyl ether (2.50 mM, 0.5 μmol) in CH_2Cl_2 was added. The final concentration of each component becomes as follows: iron(III) porphyrin (0.10 mM), TBPH (20 mM), PPAA (1.0 mM), diethyleneglycol diethyl ether (0.50 mM) in CH_2Cl_2 (1 mL). The mixture was stirred at rt. After 20 min, the reaction was quenched by adding diphenyl sulfide (4.0 mM in CH_2Cl_2, 0.5 mL, 2.0 μmol), and the mixture was stirred for 5 min. The products were quantified with referring to the internal standard (diethyleneglycol diethyl ether) by gas chromatography. The data are listed in Table 1.

2.4.2. Hydroxylation of adamantane with PPAA

Adamantane (27.2 mg, 200 μmol) and iron(III) porphyrin (0.10 μmol) was placed in a test tube fitted with a rubber septum. The inside was replaced with Ar atmosphere. A mixture (0.2 mL) of PPAA (5.0 mM, 1.0 μmol) and diethyleneglycol diethyl ether (2.50 mM, 0.5 μmol) in CH_2Cl_2 was added. The final concentration of each component becomes as follows: iron(III) porphyrin (0.10 mM), adamantane (200 mM), PPAA (1.0 mM), diethyleneglycol diethyl ether (0.50 mM) in CH_2Cl_2 (1 mL). The mixture was stirred at rt. After 20 min, the reaction was quenched by adding diphenyl sulfide (4.0 mM in CH_2Cl_2, 0.5 mL, 2.0 μmol), and the mixture was stirred for 5 min. The products were quantified with referring to the internal standard (diethyleneglycol diethyl ether) by gas chromatography. The data are listed in Table 2.

2.5. 1MeIm titration to ImTPFPP–Fe(III)Cl in acetonitrile

2.5.1. UV–vis measurements

ImTPFPP–Fe(III)Cl solution in acetonitrile (2.8×10^{-5} M, 4.0 mL) was placed in a quartz glass cuvette (band path 1 cm), and 1-methylimidazole (**1MeIm**) (0–70 eq.) was added to the solution. Each mixture was stirred for 2 min at rt and UV–vis spectrum of the solution was measured. The spectra are shown in Fig. 4.

2.5.2. NMR measurements

ImTPFPP–Fe(III)Cl solution in acetonitrile-d_3 (1.0×10^{-2} M, 0.5 mL) was placed in an NMR tube, and **1MeIm** (1, 2, and 5 eq.) was added to the solution. Each

Table 1
TBPH oxidation with PPAA catalysed by iron porphyrins[a]

Run	Catalyst	1MeIm (eq.)	$Ph_2S{=}O$ (yield, %)	Products (yield, %)		
				PAA	PhCHO	$PhCH_2OH$
1	ImTPFPP–Fe(III)Cl	0	0	88	0	4.8
2	TPFPP–Fe(III)Cl	0	0	21	6.2	64
3	TPFPP–Fe(III)Cl	100	0	90	0	1.4
4	ImTPP–Fe(III)Cl	0	0	99	0	0
5	TPP–Fe(III)Cl	0	0	48	4.7	33
6[b]	TPP–Fe(III)Cl	0	–	9	–[c]	24
7	TPP–Fe(III)Cl	100	0	90	0	0
8	ImTMP–Fe(III)Cl	0	0	96	0	1.4
9	TMP–Fe(III)Cl	0	0	55	4.4	30
10	TMP–Fe(III)Cl	100	0	90	0	1.0
11	ImTPP–Fe(III)ClO_4	0	0	95	1.2	2.5
12	TPP–Fe(III)ClO_4	0	0	64	8.7	23
13	TPP–Fe(III)ClO_4	100	0	98	0.9	0.5

[a] These reactions were carried out in CH_2Cl_2 at 25 °C under argon for 20 min. [Fe(Por)] = 0.10 mM; [PPAA] = 1.0 mM; [TBPH] = 20 mM.
[b] Reported in Ref. 3d, this reaction was carried out in benzene at 25 °C under argon for 10 min. [Fe(Por)] = 0.10 mM; [PPAA] = 1.0 mM; [TBPH] = 10 mM.
[c] No benzaldehyde, but toluene (61%) was detected. Yields are determined by GC based on PPAA.

Table 2
Hydroxylation of adamantane with PPAA by iron porphyrin catalysis[a]

Run	Catalyst	1MeIm (eq.)	Ph_2S=O (yield, %)	Products (yield, %)			Products (yield, %)		
				PAA	PhCHO	$PhCH_2OH$	1-ol	2-ol	Total
1	ImTPFPP–Fe(III)Cl	0	0	88	5.3	1.6	65	11	70
2	TPFPP–Fe(III)Cl	0	95	97	0	0	4.9	0	4.9
3	TPFPP–Fe(III)Cl	100	0	96	2.7	0.5	22	4.2	26
4	ImTPP–Fe(III)Cl	0	0	67	8.1	2.4	29	4.2	33
5	TPP–Fe(III)Cl	0	0	57	19	6.0	13	1.8	15
6[b]	TPP–Fe(III)Cl	0	–	–	13[c]	–[c]	11	2	13
7	TPP–Fe(III)Cl	100	0	91	2.7	0.6	18	2.1	20
8	ImTMP–Fe(III)Cl	0	0	75	14	5.4	19	4.6	24
9	TMP–Fe(III)Cl	0	0	60	25	10	28	8.6	37
10	TMP–Fe(III)Cl	100	0	88	5.8	0.8	8.5	1.8	10
11	ImTPP–Fe(III)ClO_4	0	0	93	6.2	0.6	46	10	56
12	TPP–Fe(III)ClO_4	0	0	66	21	8.7	15	2.6	18
13	TPP–Fe(III)ClO_4	100	0	91	7.3	0.9	12	1.2	13

[a] These reactions were carried out in CH_2Cl_2 at 25 °C under argon for 20 min. [Fe(Por)] = 0.10 mM; [PPAA] = 1.0 mM; [adamantane] = 200 mM.
[b] Reported in Ref. 3d, this reaction was carried out in benzene at 25 °C under argon for 10 min. [Fe(Por)] = 1.0 mM; [PPAA] = 1.0 mM; [adamantane] = 500 mM.
[c] Sum of benzaldehyde and benzylalcohol; yields are determined by GC based on PPAA.

mixture was kept standing for 2 min at rt and ^1H and ^{19}F NMR spectra were measured. The spectra are shown in Figs. 5 and 6. In the absence of **1MeIm**: ^1H NMR (600 MHz, acetonitrile-d_3) δ −5.4 (br-s, 3H, Im-Me), 10.5 (s, 1H, Im-H), 11.0 (s, 1H, Im-H), 80.7 (br-s, 2H, pyrrole), 81.6 (br-s, 2H, pyrrole), 82.8 (br-s, 2H, pyrrole), 83.1 (br-s, 2H, pyrrole); ^{19}F NMR (564 MHz, acetonitrile-d_3) δ −160.8 (m, 6F, phenyl-*m*), −154.3 (s, 1F, phenyl-*p*), −154.1 (s, 2F, phenyl-*p*), −127.6 (br-s, 6F, phenyl-*o*). After adding 5 eq. of **1MeIm**: ^1H NMR (600 MHz, acetonitrile-d_3) δ −19.1 (s, 2H, pyrrole), −15.4 (s, 2H, pyrrole), −14.4 (s, 2H, pyrrole), −8.0 (br-s, 2H, pyrrole), 19.8 (s, 3H, 1MeIm-Me), 20.0 (s, 3H, 1MeIm-Me); ^{19}F NMR (564 MHz, acetonitrile-d_3) δ −165.98 (m, 2F, phenyl-*m*), −165.63 (dd, J = 18.6, 18.6 Hz, 2F, phenyl-*m*), −165.43 (dd, J = 18.6, 18.6 Hz, 2F, phenyl-*m*), −156.95 (t, J = 18.6 Hz, 1F, phenyl-*p*), −156.50 (t, J = 18.6 Hz, 2F, phenyl-*p*), −143.59 (d, J = 18.6 Hz, 1F, phenyl-*o*), −142.47 (d, J = 18.6 Hz, 1F, phenyl-*o*), −142.19 (d, J = 18.6 Hz, 2F, phenyl-*o*), −141.91 (d, J = 18.6 Hz, 2F, phenyl-*o*).

3. Results

3.1. Synthesis of iron(III) porphyrins

Three chloro(imidazolylporphyrinato)iron(III)s having tripentafluorophenyl, triphenyl, and trimesityl (tri(2,4,6-trimethylphenyl)) groups as *meso*-substituents were newly prepared as oxidation catalysts. The pentafluorophenyl group is highly electron-deficient, whereas the mesityl group is electron donating compared with the phenyl group. Therefore, the electronic effect of the peripheral aryl groups can be examined using these three porphyrins. The free base porphyrins, **ImTPFPPH$_2$** and **ImTPPH$_2$**, were synthesized by condensation of imidazolecarboxaldehyde, pyrrole, and the corresponding arylaldehyde (Adler's method). Pure **ImTPPH$_2$** was obtained by SiO_2 chromatography. In the case of **ImTPFPPH$_2$**, however, a byproduct with the same polarity accompanied the target free base porphyrin. The pure **ImTPFPPH$_2$** was obtained by converting the free base porphyrin into its zinc complex. Because the polarity of the complementary coordination dimer of the zinc complex on TLC becomes much lower than that of the free base while the byproduct maintains its polarity, they can be easily separated by SiO_2 column chromatography. Finally, the pure free base, **ImTPFPPH$_2$**, was obtained by demetallation with hydrochloric acid solution (Scheme 1).

Synthesis of mesityl porphyrin, **ImTMPH$_2$**, is more difficult. An Adler method and a normal dipyrromethane method using one kind of acid, either BF_3 Et_2O or trifluoroacetic acid (TFA), did not give **ImTMPH$_2$**. Finally, stepwise reactions using two kinds of acid succeeded in giving the **ImTMPH$_2$**. Mesityl dipyrromethane (2 eq.) and mesitylaldehyde (1 eq.) were reacted in the presence of BF_3 Et_2O first to give a non-cyclic tetrapyrrole

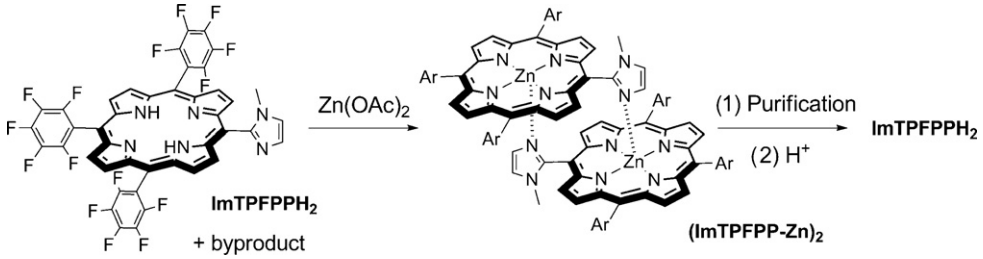

Scheme 1. Preparation of pure **ImTPFPPH$_2$**.

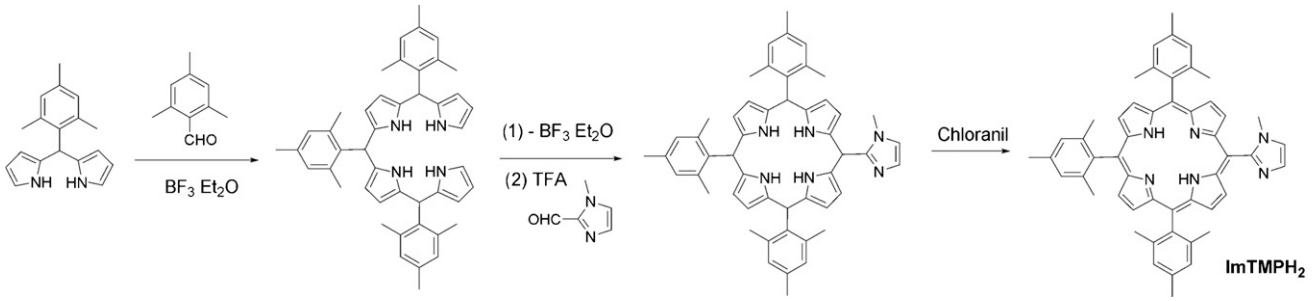

Scheme 2. Preparation of **ImTMPH$_2$**.

that had three mesityl groups. Formation of the tetrapyrrole was monitored by MALDI-TOF mass spectrometry. When the formation was almost complete, the mixture was passed through a column packed with $NaHCO_3$ to remove BF_3 Et_2O. Then, addition of imidazolecarboxaldehyde and TFA to the mixture followed by oxidation with chloranil gave **ImTMPH$_2$**. It is noteworthy that mesitylaldehyde was activated by BF_3 Et_2O but not by TFA, whereas BF_3 Et_2O deactivates imidazolecarboxaldehyde by precipitate formation. Replacing BF_3 Et_2O with TFA is essential to synthesize **ImTMPH$_2$**. Pure **ImTMPH$_2$** was obtained by a similar method to that of **ImTPFPPH$_2$** via the zinc complex (Scheme 2).

Iron(III) complexes of the free base imidazolylporphyrins were obtained by treatment with $FeCl_2$. The corresponding chloro(tetraarylporphyrinato)iron(III)s were also prepared as reference compounds for the oxidation catalyst. Iron(III) perchlorate porphyrins were prepared from the corresponding chloride complexes by treatment with $AgClO_4$ (Fig. 2).

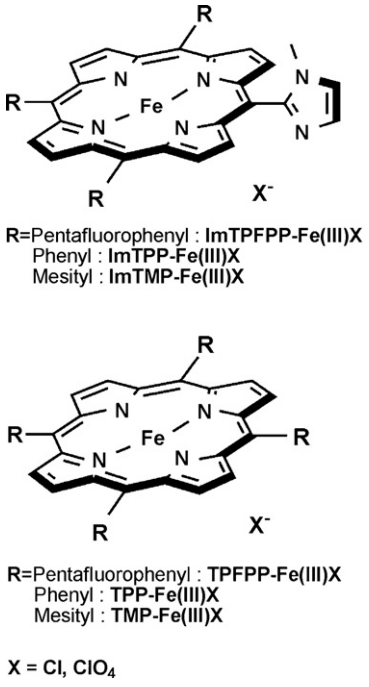

Fig. 2. Structures of porphyrins.

3.2. Heterolytic O–O bond cleavage of peroxy acid

Phenylperacetic acid (PPAA) as a ligand of iron(III) porphyrin is a sensitive probe to evaluate the pathway leading to either heterolytic or homolytic cleavage [3c,3d] (Scheme 3). It is transformed into phenylacetic acid (PAA) via a heterolytic O–O bond cleavage, whereas benzyl alcohol is produced via homolytic cleavage. Benzyl alcohol is sometimes oxidized further to benzaldehyde. Therefore, the ratio of PAA to the sum of benzyl alcohol and benzaldehyde becomes a measure of the reaction pathways leading to either heterolytic or homolytic cleavage, respectively. High-valent iron porphyrin species, compounds I and II, formed via heterolytic and homolytic cleavages, respectively, are known to be reduced by 2,4,6-tri-*t*-butylphenol (TBPH) to regenerate the starting iron(III) porphyrin. Therefore, the reaction was undertaken in the presence of a large excess of TBPH.

The reaction was carried out in the presence of iron(III) porphyrin (0.10 mM), PPAA (1.0 mM), and TBPH (20 mM) in CH_2Cl_2 under an Ar atmosphere. After 20 min, unreacted PPAA was quenched with diphenyl sulfide (Ph_2S) to determine the consumption of PPAA. The amounts of diphenylsulfoxide (Ph_2S=O), PAA, benzaldehyde, and benzyl alcohol were determined by gas chromatography. The yields based on PPAA are shown in Table 1. Three iron(III) imidazolylporphyrin

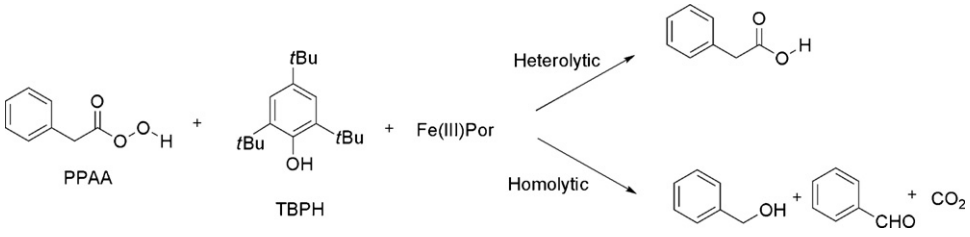

Scheme 3. Reaction pathway of PPAA and TBPH in the presence of iron(III) porphyrin.

chlorides having tri(pentafluorophenyl) (**ImTPFPP–Fe(III)Cl**, run 1), triphenyl (**ImTPP–Fe(III)Cl**, run 4), and trimesityl (**ImTMP–Fe(III)Cl**, run 8) substituents were employed. The corresponding tetraaryl iron(III) porphyrins without the imidazolyl group were used in the absence (runs 2, 5, and 9) and presence of 100 eq. of *N*-methylimidazole (runs 3, 7, and 10) for comparison. Results for the perchlorate complexes of phenyl-substituted porphyrins are listed in runs 11–13.

Because no diphenylsulfoxide was detected after 20 min for all runs, PPAA was consumed quantitatively within the initial 20 min. Three iron(III) imidazolylporphyrin chlorides gave PAA predominantly (88% for **ImTPFPP** (run 1), quantitative for **ImTPP** (run 4), 96% for **ImTMP** (run 8)) whereas significant amounts of benzyl alcohol and benzaldehyde were produced for cases of non-imidazolylporphyrins (runs 2, 5, and 9). These results indicate that heterolytic cleavage predominates for the former cases, and that considerable homolytic cleavage occurred in the latter cases. When 100 eq. of *N*-methylimidazole were added to the non-imidazolylporphyrins (runs 3, 7, and 10), the PAA formation was increased to 90% for all three cases, clearly suggesting that imidazole assists heterolytic cleavage of the O–O bond. Exchange of the counter ion by perchlorate ion has a minimal effect and maintains the product percentages of the chloride ion cases (runs 11–13 in comparison with runs 4, 5 and 7).

3.3. Catalytic oxidation of adamantane with PPAA

Oxidation of adamantane is also a sensitive probe to evaluate the characteristics of compound I formed by heterolytic O–O bond cleavage. Therefore, a mixture of adamantane (200 mM), iron(III) porphyrin (0.10 mM), and PPAA (1.0 mM) in CH_2Cl_2 was stirred under an Ar atmosphere. After 20 min, diphenyl sulfide was added to quench the remaining PPAA. Products were analysed by gas chromatography. All of the data are listed in Table 2. The most striking difference from the data of Table 1 was observed for run 2, where diphenylsulfoxide was detected almost quantitatively, suggesting almost no reaction of PPAA, even after 20 min. This result is consistent with the observation that O–O bond cleavage of the peroxo complex of electron-deficient PTFPP–Fe(III) is sluggish in the absence of imidazole [14], and the direct hydroxylation of adamantane with the peroxo complex is also slow, unlike epoxidation of alkenes [3e]. Increasing the electron-donating character of the porphyrin ligand promotes O–O bond cleavage by the "push effect". Thus, the yields of adamantanols increase in the order of electron-donating character of the peripheral aryl groups (TPP–FeCl (run 5) < TMP–FeCl (run 9)). In the presence of an external imidazole ligand with TPFPP–FeCl, PPAA was consumed completely within 20 min, predominantly through a heterolytic cleavage mechanism (run 3). This is consistent with previous reports claiming the importance of the push effect by a proximal ligand [3d,14]. Although the heterolytic cleavage was dominant in run 3, conversion of adamantane oxidation was only 26%. In the case of **ImTPFPP–Fe(III)Cl** (run 1), the yield of heterolytic cleavage corresponds almost to the conversion of adamantane oxidation. This result indicates that most of compound I in run 1 is active as the oxidant of adamantane, and the minimal imidazolyl ligand attached to the porphyrin is effective as the electron-deficient system to make this system the best among those investigated. When **ImTPP–Fe(III)Cl** and **ImTMP–Fe(III)Cl** are used, smaller percentages of heterolytic cleavage lead to adamantane oxidation (runs 4 and 8). In contrast to the tetraaryl cases (runs 2, 5, and 9), yields of adamantanols decrease by increased electron donation from aryl substituents (run 4 vs. run 8). These results suggest that the coordination from the imidazole substituent becomes less significant for cases where electron density of the central iron(III) is increased by the push effect from the peripheral aryl groups. The favourable effect of imidazole substitution is lost for the TMP cases (run 8 vs. run 9), where the peripheral mesityl substituents have the dominant effect of electron donation to the central iron(III). When perchlorate ion was used as the counter ion instead of chloride ion for **ImTPP**, the conversion increased to 56% from 33%, suggesting that iron(III) porphyrin of cationic nature is a better catalyst (run 11 vs. run 4). Addition of external *N*-methylimidazole (100 eq.) to any type of iron(III) tetraarylporphyrin does not improve the oxidation of adamantane very much, even though heterolytic cleavage becomes dominant. Apparently, other pathways make significant contributions to the consumption of compound I in the presence of excess imidazole.

In the following sections, we will analyse the structure of **ImTPFPP–Fe(III)Cl** in detail using UV–vis and NMR spectra.

3.4. UV–vis study of ImTPFPP–Fe(III)Cl

UV–vis spectra of **ImTPFPP–Fe(III)Cl** and **TPFPP–Fe(III)Cl** in acetonitrile are shown in Fig. 3. The latter spectrum is typical of Fe(III)Cl porphyrin, which has an LMCT band at 350 nm and a Soret band at 408 nm. The spectrum of **ImTPFPP–Fe(III)Cl**, however, shows a broad Soret band at 395 nm without showing an LMCT band. The characteristic broad Soret band is similar to those observed for complementary dimers of Co(III) imidazolylporphyrin [8] and Rh(III) pyridylporphyrin [15]. To confirm the formation of the dimeric structure, *N*-methylimidazole was titrated into the solution (Fig. 4). The broad Soret band was red-shifted and

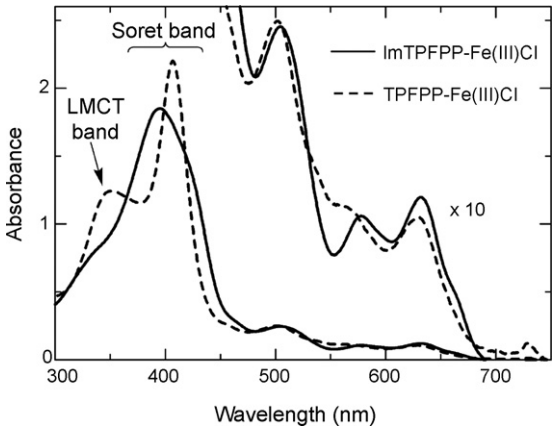

Fig. 3. UV–vis spectra of **ImTPFPP–Fe(III)Cl** (solid line) and **TPFPP–Fe(III)Cl** (doted line) in acetonitrile at rt. Cell length = 1 cm.

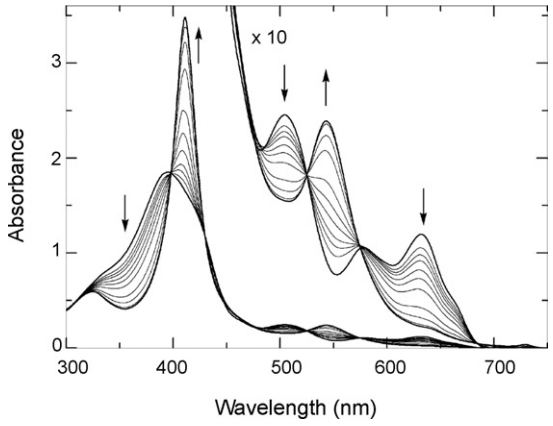

Fig. 4. UV–vis spectral change of **ImTPFPP–Fe(III)Cl** dimer to monomer on the addition of **1MeIm** in acetonitrile (**ImTPFPP–Fe(III)Cl**: 2.8×10^{-5} M, **1MeIm**: from 0 to 70 eq.).

sharpened, and the Q-bands also changed, passing through isosbestic points. The converged spectrum was almost identical with the 6-coordinating complex prepared by the addition of *N*-methylimidazole to **TPFPP–Fe(III)Cl** in acetonitrile. These results suggest that the original acetonitrile solution of **ImTPFPP–Fe(III)Cl** is composed predominantly of a complementary 5-coordinating dimer.

The original spectrum of **ImTPFPP–Fe(III)Cl** (2.8×10^{-5} M in acetonitrile) converged to the final spectrum after the addition of 70 eq. of *N*-methylimidazole. If we assume the following equilibria and complete dimer formation at the initial state [16], the self-association constant of **ImTPFPP–Fe(III)Cl**, K_0, is estimated from competitive coordination experiments

$$2\mathrm{P} \rightleftarrows \mathrm{P}_2 \qquad K_0 = \frac{[\mathrm{P}_2]}{[\mathrm{P}]^2} \tag{1}$$

$$\mathrm{P} + 2\mathrm{L} \rightleftarrows \mathrm{PL}_2 \qquad K_\mathrm{a} = \frac{[\mathrm{PL}_2]}{[\mathrm{P}][\mathrm{L}]^2} \tag{2}$$

$$\mathrm{P}_2 + 4\mathrm{L} \rightleftarrows 2\mathrm{PL}_2 \qquad K_\mathrm{b} = \frac{[\mathrm{PL}_2]^2}{[\mathrm{P}_2][\mathrm{L}]^4} \tag{3}$$

$$K_0 = \frac{K_\mathrm{a}^2}{K_\mathrm{b}} \tag{1}$$

where P, P_2, L, and PL_2 are the monomeric chloride complex, dimer, imidazole, and 6-coordinated bisimidazole complex, respectively.

K_a' ($9.12 \times 10^7\ \mathrm{M}^{-2}$) obtained by the titration of *N*-methylimidazole into TPFPP–Fe(III)Cl may represent the approximate value of K_a [17]. K_b was obtained as $5.75 \times 10^9\ \mathrm{M}^{-3}$ from the above titration experiment of **ImTPFPP–Fe(III)Cl**. Then, K_0 was calculated to be $1.45 \times 10^6\ \mathrm{M}^{-1}$. This is much smaller than the extremely large equilibrium constant of zinc imidazolylporphyrins ($K_0 > 10^{11}\ \mathrm{M}^{-1}$) [18], but large enough to maintain the dimeric structure in dilute micromolar solutions. Probably, charge repulsion between the two cationic Fe(III) porphyrins in the dimer contributes to the decrease in the self-association constant.

The characteristic UV–vis spectrum of the dimer from **ImTPFPP–Fe(III)Cl** was observed only in acetonitrile (ε (dielectric constant [19]) 36.64). In dioxane (ε 2.21), benzene (ε 2.28), chloroform (ε 4.81), ethyl acetate (ε 6.08), THF (ε 7.52), acetone (ε 21.0), and benzonitrile (ε 25.9), spectral patterns were similar to that of TPFPP–Fe(III)Cl and regarded as representing predominantly the monomeric chloro complex. In methanol (ε 32.35) and DMF (ε 37.06), monomeric 6-coordinated complexes coordinated by the two solvent molecules were observed. In addition, **ImTPP–Fe(III)Cl** and **ImTMP–Fe(III)Cl** exist as monomeric forms, even in acetonitrile. Aryl substituents and solvent strongly affect the dimer formation tendency. This will be discussed later.

3.5. ^{1}H and ^{19}F NMR study of ImTPFPP–Fe(III)Cl

^{1}H and ^{19}F NMR spectra of **ImTPFPP–Fe(III)Cl** in CD_3CN (10 mM as a monomeric unit) are shown in Figs. 5 and 6. In the ^{1}H NMR spectra, characteristic β proton signals appeared in the region 90–70 ppm, which correspond to the high-spin state of Fe(III) porphyrin [20]. Imidazolyltriarylporphyrin generally shows three kinds of β protons: those nearest to the imidazolyl group, the next nearest, and the others, in a 1:1:2 ratio. Therefore, Fig. 5a seems to include two kinds of species, three major peaks at 83.0, 81.6, and 80.7 ppm (marked as **x**) and minor peaks at 75.8 and 73.8 ppm (filled circles) (the other is probably overlapped with the major peaks). In the ^{19}F NMR spectra, the two species are separated more clearly. The major peaks appear around −128, −154.2, and 161 ppm, and the minor ones around −108, −155, and −162 ppm. Judging from the characteristic ortho fluorine signal at −108 ppm, the latter is assigned as the peak of monomeric Fe(III)Cl–porphyrin. Therefore, the former peak is assigned temporarily as the 5-coordinating dimer. When 1 eq. of 1-methylimidazole was added to the mixture, the major signals disappeared; however, the minor ones remained in both the ^{1}H and the ^{19}F NMR spectra (Figs. 5b and 6b). Instead of the major peaks, peaks due to low-spin species appeared at −8.0, −14.4, −15.4, and −19.1 ppm (β-Hs) in the ^{1}H NMR spectra and −141.9 (*o*), −142.2 (*o*), −142.5 (*o*), −143.6 (*o*), −156.5 (*p*), −157.0 (*p*), and −165.4 (*m*), −165.6 (*m*), −166.0 (*m*) in the ^{19}F NMR spectra. All of the signals were converted finally to a new species (open circles) after the addition of 5 eq. of 1-methylimidazole. The new species is assigned as a monomeric 6-coordinated bisimidazole adduct. ^{19}F NMR spectra also show the conversion of high-spin species into the bisimidazole adduct. All NMR and UV–vis absorption spectra and titration experiments with 1-methylimidazole consistently lead to the conclusion that **ImTPFPP–Fe(III)Cl** exists as a predominantly high-spin dimer in acetonitrile, as shown in Fig. 1.

4. Discussion

4.1. Formation of 5-coordinating Fe(III) porphyrin complex

Iron(III) porphyrin pentacoordinated with an imidazole derivative has been claimed to be an active form of various cytochromes for performing enzymatic reactions [21]. How-

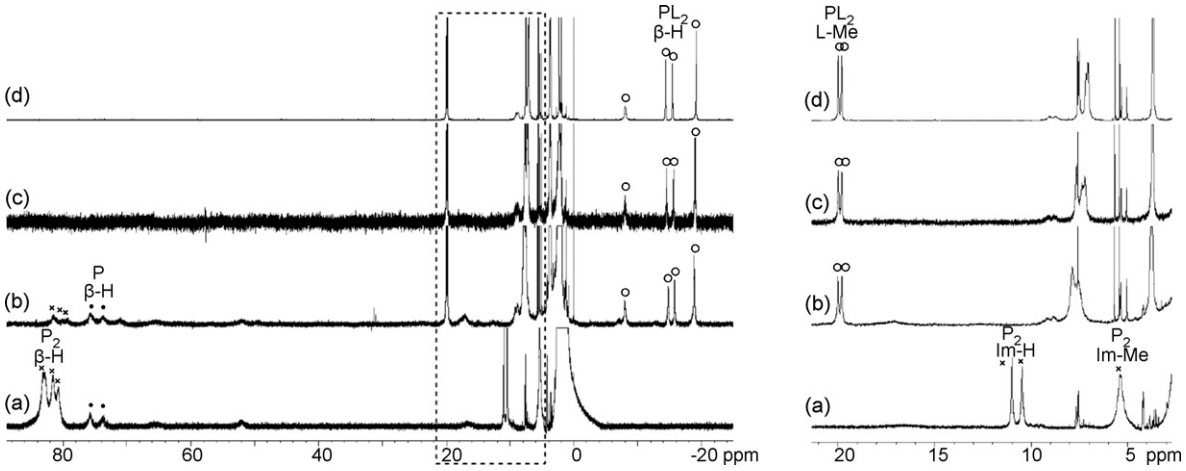

Fig. 5. ^{1}H NMR (600 MHz) spectral change of **ImTPFPP–Fe(III)Cl**: 1.0×10^{-2} M taken in acetonitrile-d_3 solution at the addition of various amounts of **1MeIm**: (a) 0.0 eq.; (b) 1.0 eq.; (c) 2.0 eq.; (d) 5.0 eq. Marks **x**, filled circle, and open circle were assigned as 5-coordinating **ImTPFPP–Fe(III)** porphyrin dimer, **ImTPFPP–Fe(III)Cl**, and 6-coordinated bisimidazole adduct of **ImTPFPP–Fe(III)** porphyrin, respectively.

ever, the 5-coordinated complex was obtainable under restricted conditions of controlled supply of ligands from environmental peptide side chains, as in enzymatic systems. Synthesis of such a complex is not easy in homogeneous media because the association constant of the sixth coordination of imidazole is larger than that of the fifth coordination. Even the addition of 1 eq. of imidazole to chloro(porphyrinatoiron(III)) produces a 1:1 mixture of 6-coordinated bisimidazole adduct and starting chloro complex. Nakamura reported selective synthesis of mono(imidazole)-ligated (*meso*-tetramesitylporphyrinato)iron(III) using a weakly coordinating anion such as perchlorate ion (ClO_4^-) instead of chloride ion. In their method, bulky substituents on imidazole and the peripheral four aryl groups are essential [22]. As a coordination ligand, 4,5-dichloroimidazole and 2-alkylimidazoles, such as 2-(*i*-propyl)imidazole and 2-ethylimidazole, were effective, but too bulky 2-(*tert*-butyl)imidazole did not give the corresponding 5-coordinated complex. In our present case, 5-coordinated iron(III) porphyrin was derived from the chloride form, and the bulky mesityl group was rather catalytically ineffective. Therefore, the method suggests a new strategy for constructing a catalytically active 5-coordinated complex by dimerization. Because acetonitrile and pentafluorophenyl groups are essential to obtain the 5-coordinated dimer, synthetic conditions for the dimer formation are still limited. A delicate balance between the affinity of counter anion and imidazole substituent is still important as the environmental conditions. Probably, polar acetonitrile effectively solvates the chloride ion, but does not coordinate the cationic iron(III) porphyrin. The more coordinating methanol and DMF act as competing ligands towards imidazole in the presence of a large excess and prevent the dimerization. It is noted that it is not essential for the catalytic reaction to keep the 5-coordinated dimer structure as the dominant species. Although no dimer structure was observed in CH_2Cl_2 by UV–vis spectroscopy, the effect of the

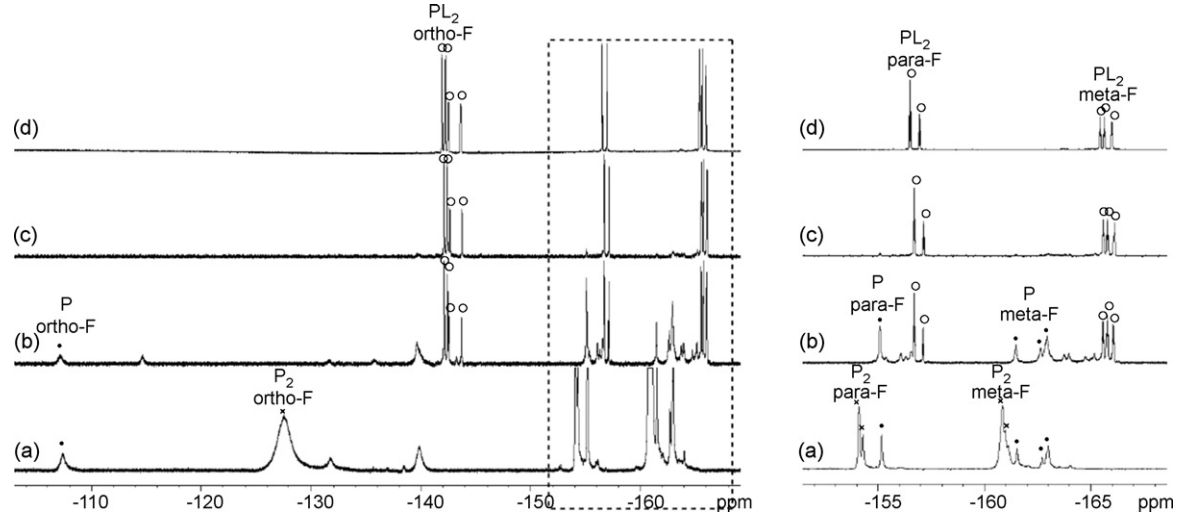

Fig. 6. ^{19}F NMR (564 MHz) spectral change of **ImTPFPP–Fe(III)Cl**: 1.0×10^{-2} M taken in acetonitrile-d_3 solution on the addition of various amounts of **1MeIm**: (a) 0.0 eq.; (b) 1.0 eq.; (c) 2.0 eq.; (d) 5.0 eq. Marks **x**, filled circle, and open circle were assigned as 5-coordinating **ImTPFPP–Fe(III)** porphyrin dimer, **ImTPFPP–Fe(III)Cl**, and 6-coordinated bisimidazole adduct of **ImTPFPP–Fe(III)** porphyrin, respectively.

imidazolyl group was clearly operative in the catalytic oxidation in CH_2Cl_2. Unfortunately, catalytic oxidation of TBPH and adamantane could not be undertaken in acetonitrile because of the low solubility of the substrates.

4.2. Activity of catalyst

An efficient push effect by the proximal imidazole and thiolate ligands has been claimed to be important in heterolytic O–O bond cleavage reactions [23]. In fact, the addition of 100 eq. of external *N*-methylimidazole improves yields of PAA, as shown in Tables 1 and 2. However, yields of adamantanols were inferior to those of heterolytic cleavage. This suggests that excess imidazole inhibits the oxidation reaction somewhere in the catalytic cycle. A great advantage of the use of imidazolyl-appended iron(III) porphyrin results from the point that exactly 1 eq. of imidazole is enough to coordinate because of its strong coordination by complementarity. Therefore, high percentages of consumed PPAA successfully oxidized adamantane. Imidazole effect was reported by Nam in catalytic epoxydation of cyclohexene with H_2O_2 in the presence of (*meso*-tetraarylporphyrinato)iron(III) [24]. The yields of oxidized product depend strongly on the electron-donating ability of the added imidazoles, and 5-chloro-1-methylimidazole showed the best performance. Considering with Nakamura's report [21], both electron-donating ability and bulkiness of imidazole are important factors. Performance of catalytic oxidation in our system may be modified further by introduction of a substituent on the imidazolyl part.

Halogenated catalysts are known as oxidation-resistant materials [5]. Turnover numbers in the catalytic oxidation are generally larger than for the corresponding non-fluorinated catalysts. Furthermore, **ImTPFFP–Fe(III)Cl** can be prepared easily from commercially available products. This is another advantage from the synthetic viewpoint. These considerations suggest **ImTPFFP–Fe(III)Cl** as an interesting oxidation catalyst.

5. Conclusion

Using the probe reaction of adamantane oxidation with PPAA, the catalytic ability of imidazolyl-appended iron(III) porphyrins was examined. **ImTPFPP–Fe(III)Cl** showed the best performance in producing adamantanols. From the comparison among different iron(III) porphyrins, we conclude that the pentafluorophenyl groups in **ImTPFPP–Fe(III)Cl** have two roles: (1) the electron-withdrawing nature decreases the electron density of the central iron(III) making it more amenable to accepting imidazolyl ligation, which assists the cleavage of O–O bond of phenylperacetate ligand to generate the active high-valent oxo-iron species; and (2) halogenation substitution increases resistance to decomposition by the high-valent oxo-iron species.

The imidazolyl ligation was directly observed spectroscopically using UV–vis as well as ^1H and ^{19}F NMR as the complementary dimer of **ImTPFPP–Fe(III)Cl** in acetonitrile. Stable formation of the dimer is highly solvent dependent. Only in acetonitrile was a clear dimer structure observed; however, the monomeric chloride complex was dominant in CH_2Cl_2 in which hydroxylation of adamantane was performed. This result indicates that it is not very important to keep the dimer structure in the whole catalytic cycle, and ligation of the transient species in the catalytic cycle is active for the reaction. Complementary coordination is concluded to be a unique method to perform a single imidazolyl ligation to iron(III) porphyrin.

Acknowledgements

This work was supported by Young Scientists (B) (17750091) (AS) and Grants-in-Aid for Scientific Research (A) (YK) from the Japan Society for the Promotion of Science (JSPS).

Appendix A. Supplementary data

Supplementary data associated with this article can be found, in the online version, at doi:10.1016/j.molcata.2007.12.016.

References

[1] (a) P.R. Ortiz de Montellano, Cytochrome P450: Structure, Mechanism, and Biochemistry, 3rd ed., Kluwer Academic/Plenum Publishers, New York, 2005;
(b) I.G. Denisov, T.M. Makris, S.G. Sligar, I. Schlichting, Chem. Rev. 105 (2005) 2253;
(c) B. Meunier, S.P. de Visser, S. Shaik, Chem. Rev. 104 (2004) 3947;
(d) M.M. Abu-Omar, A. Loaiza, N. Hontzeas, Chem. Rev. 105 (2005) 2227;
(e) M. Costas, M.P. Mehn, M.P. Jensen, L. Que, Chem. Rev. 104 (2004) 939;
(f) J.T. Groves, J. Inorg. Biochem. 100 (2006) 434;
(g) X. Shan, J.L. Que, J. Inorg. Biochem. 100 (2006) 421.
[2] (a) A. Henriksen, A.T. Smith, M. Gajhede, J. Biol. Chem. 274 (1999) 35005;
(b) T.L. Poulos, B.C. Finzel, A.J. Howard, J. Mol. Biol. 195 (1987) 687.
[3] (a) W.D. Woggon, Acc. Chem. Res. 38 (2005) 127;
(b) Y. Watanabe, H. Nakajima, T. Ueno, Acc. Chem. Res. 40 (2007) 554;
(c) T.G. Traylor, W.A. Lee, D.V. Stynes, J. Am. Chem. Soc. 106 (1984) 755;
(d) T. Higuchi, K. Shimada, N. Maruyama, M. Hirobe, J. Am. Chem. Soc. 115 (1993) 7551;
(e) N. Suzuki, T. Higuchi, T. Nagano, J. Am. Chem. Soc. 124 (2002) 9622;
(f) K.A. Lee, W. Nam, J. Am. Chem. Soc. 119 (1997) 1916;
(g) W. Nam, Acc. Chem. Res. 40 (2007) 522;
(h) W. Nam, H.J. Lee, S.Y. Oh, C. Kim, H.G. Jang, J. Inorg. Biochem. 80 (2000) 219.
[4] S. Ozaki, M.P. Roach, T. Matsui, Y. Watanabe, Acc. Chem. Res. 34 (2001) 818.
[5] (a) E. Takahashi, H. Amatsu, T.K. Miyamoto, Y. Sasaki, Nippon Kagaku Kaishi (1988) 480;
(b) Y. Iamamoto, M.D. Assis, K.J. Ciuffi, H.C. Sacco, L. Iwamoto, A.J.B. Melo, O.R. Nascimento, C.M.C. Prado, J. Mol. Catal. A: Chem. 109 (1996) 189;
(c) R. Iwanejko, P. Battioni, D. Mansuy, T. Mlodnicka, J. Mol. Catal. A: Chem. 111 (1996) 7.
[6] Y. Kobuke, H. Miyaji, J. Am. Chem. Soc. 116 (1994) 4111.
[7] Y. Kobuke, H. Miyaji, Bull. Chem. Soc. Jpn. 69 (1996) 3563.
[8] Y. Inaba, Y. Kobuke, Tetrahedron 60 (2004) 3097.
[9] R.N. McDonald, R.N. Steppel, J.E. Dorsey, Org. Synth. 52 (1978) 166.
[10] F.R. Longo, M.G. Finarelli, J.B. Kim, J. Heterocycl. Chem. 6 (1969) 927.
[11] A.D. Adler, F.R. Longo, J.D. Finarelli, J. Goldmacher, J. Assour, L. Korsakoff, J. Org. Chem. 32 (1967) 476.
[12] J.S. Lindsey, R.W. Wagner, J. Org. Chem. 54 (1989) 828.
[13] C. Lee, J.S. Lindsey, Tetrahedron 50 (1994) 11427.
[14] K. Yamaguchi, Y. Watanabe, I. Morishima, J. Chem. Soc. Chem. Commun. (1992) 1709.

[15] K. Fukushima, K. Funatsu, A. Ichimura, Y. Sasaki, M. Suzuki, T. Fujihara, K. Tsuge, T. Imamura, Inorg. Chem. 42 (2003) 3187.
[16] NMR study described later indicates the existence of minor monomeric chloro complex. However, clear isosbestic points in the UV–vis titration strongly suggest that dimer is dominant under the conditions.
[17] The value K'_a approximated from TPFPP–Fe(III)Cl may be larger than the real K_a because of the different number of electron deficient pentafluorophenyl groups. Therefore, the obtained K_0 includes some error.
[18] D. Furutsu, A. Satake, Y. Kobuke, Inorg. Chem. 44 (2005) 4460.
[19] J.A. Dean (Ed.), Lange's Handbook of Chemistry, 15th ed., McGraw-Hill, New York, 1999.
[20] N.L. Mar, F.A. Walker, J. Am. Chem. Soc. 94 (1972) 8607.
[21] P.C. Weber, R.G. Bartsch, M.A. Cusanovich, R.C. Hamlin, A. Howard, S.R. Jordan, M.D. Kamen, T.E. Meyer, D.W. Weatherford, N.h. Xuong, F.R. Salemme, Nature 286 (1980) 302.
[22] (a) A. Ikezaki, M. Nakamura, Inorg. Chem. 41 (2002) 6225;
(b) A. Ikezaki, M. Nakamura, J. Inorg. Biochem. 84 (2001)137.
[23] T. Higuchi, S. Uzu, M. Hirobe, J. Am. Chem. Soc. 112 (1990) 7051.
[24] W. Nam, H.J. Han, S.Y. Oh, Y.J. Lee, M.H. Choi, S.Y. Han, C. Kim, S.K. Woo, W. Shin, J. Am. Chem. Soc. 122 (2000) 8677.